Article

Gold Nanoparticles in Biology: Beyond Toxicity to Cellular Imaging

Catherine J. Murphy, Anand M. Gole, John W. Stone, Patrick N. Sisco, Alaaldin M. Alkilany, Edie C. Goldsmith, and Sarah C. Baxter

Acc. Chem. Res., **Article ASAP** • DOI: 10.1021/ar800035u

ACCOUNTS
of chemical research

Gold Nanoparticles in Biology: Beyond Toxicity to Cellular Imaging

CATHERINE J. MURPHY,*,† ANAND M. GOLE,†
JOHN W. STONE,† PATRICK N. SISCO,†
ALAALDIN M. ALKILANY,† EDIE C. GOLDSMITH,§ AND
SARAH C. BAXTER‡

†Department of Chemistry and Biochemistry, University of South Carolina, Columbia, South Carolina 29208, ‡Department of Mechanical Engineering, University of South Carolina, Columbia, South Carolina 29208, §Department of Cell and Developmental Biology and Anatomy, University of South Carolina School of Medicine, Columbia, South Carolina 29208

RECEIVED ON FEBRUARY 1, 2008

CONSPECTUS

Gold, enigmatically represented by the target-like design of its ancient alchemical symbol, has been considered a mystical material of great value for centuries. Nanoscale particles of gold now command a great deal of attention for biomedical applications. Depending on their size, shape, degree of aggregation, and local environment, gold nanoparticles can appear red, blue, or other colors. These visible colors reflect the underlying coherent oscillations of conduction-band electrons ("plasmons") upon irradiation with light of appropriate wavelengths. These plasmons underlie the intense absorption and elastic scattering of light, which in turn forms the basis for many biological sensing and imaging applications of gold nanoparticles. The brilliant elastic light-scattering properties of gold nanoparticles are sufficient to detect individual nanoparticles in a visible light microscope with $\sim 10^2$ nm spatial resolution.

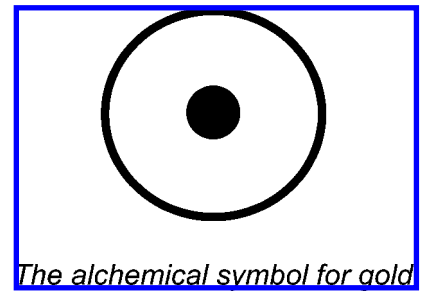
The alchemical symbol for gold

Despite the great excitement about the potential uses of gold nanoparticles for medical diagnostics, as tracers, and for other biological applications, researchers are increasingly aware that potential nanoparticle toxicity must be investigated before any *in vivo* applications of gold nanoparticles can move forward. In this Account, we illustrate the importance of surface chemistry and cell type for interpretation of nanoparticle cytotoxicity studies. We also describe a relatively unusual live cell application with gold nanorods. The light-scattering properties of gold nanoparticles, as imaged in dark-field optical microscopy, can be used to infer their positions in a living cell construct. Using this positional information, we can quantitatively measure the deformational mechanical fields associated with living cells as they push and pull on their local environment. The local mechanical environment experienced by cells is part of a complex feedback loop that influences cell metabolism, gene expression, and migration.

Introduction

Gold has been the object of long-standing fascination for its supposed ancient medicinal value and for its ornamental value.[1−3] "Red gold" for stained glass was known to medieval artisans to be "finely-divided" gold, dispersed in plain glass.[1−4] Michael Faraday's samples of "colloidal gold", which he made in solution are still on display at the Faraday Museum, London.[3] We now know that nanoscale (~100 nm or less) particles of gold are responsible for these brilliant colors.

What makes nanoparticulate gold appear red or purple or colors other than the "gold" of its bulk counterpart? The quantitative answer is in some ways surprisingly complicated,[5] but qualitatively the picture is reasonably clear. In the range of ~5−200 nm in diameter, gold nanoparticles are

10.1021/ar800035u CCC: $40.75

SCHEME 1. Pie Chart Depicting the Different Biomedical Applications of Gold Nanoparticles[a]

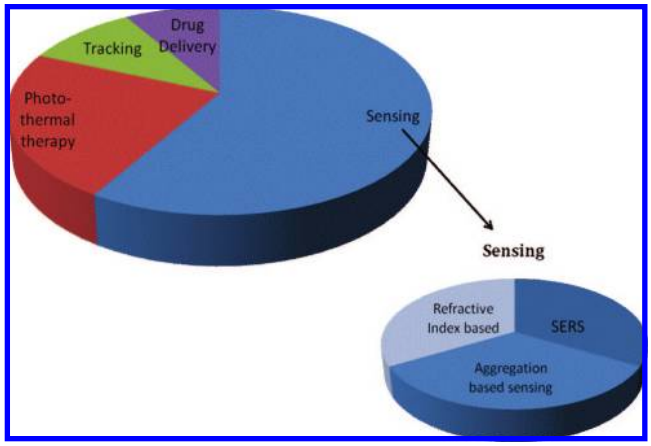

[a] Pie slice sizes roughly correspond to the length of time that there is literature in the area (e.g., sensing since the 1970s, tracking and photothermal therapy since the early 2000s). Chemical sensing can be based on particle aggregation, changes in local refractive index due to chemical binding, or surface-enhanced Raman scattering (SERS) due to inelastic scattering of light from vibrations in molecules near the surface. Tracking of nanoparticles in a complex biological system is possible using dark-field optical microscopy or two-photon luminescence microscopy. Therapeutic applications of gold nanoparticles (drug delivery and photothermal therapy, wherein gold nanoparticles rapidly release heat into their local environment upon light absorption) are discussed in other Accounts in this issue.

large enough to support a conduction band, are comparable to the mean free path of electrons in the metal at room temperature (~100 nm), but are rather small compared with the wavelengths of visible light (~400−750 nm). Irradiation with light at certain frequencies results in a collective oscillation of electrons known as "plasma oscillations" or "plasmons"[6] that are generally pictured as washing over the surface of the particle ("surface plasmons" or "localized surface plasmon resonance", LSPR). The optical properties of small metal nanoparticles are dominated by such collective oscillations that are in resonance with the incident electromagnetic radiation. For gold, it happens that the resonance frequency of this oscillation, governed by its bulk dielectric constant, lies in the visible region of the electromagnetic spectrum.[6]

Because nanoparticles have a high surface area to volume ratio, the plasmon frequency is exquisitely sensitive to the dielectric (refractive index) nature of its interface with the local medium. Any changes to the surroundings of these particles (surface modification, aggregation, medium refractive index, etc.) leads to colorimetric changes of the dispersions.[4−9] Particle aggregation leads to the coupling of plasmons, with a concomitant shifting of plasmon frequencies, resulting in a surface sensitivity that has been widely used for chemical sensing (Scheme 1), assuming that particle aggregation is controlled by surface chemistry.[7,8] Not only is light strongly absorbed by plasmons, it is also Rayleigh (elastically) scattered by them, and as the particle gets larger, a larger proportion of the outgoing light is scattered, compared with that absorbed.[5] Because the light scattered from gold nanoparticles is in the visible portion of the electromagnetic spectrum in accord with their plasmon bands, it is possible to optically track the position of individual nanoparticles, paving the way for imaging applications (Scheme 1).

In the past decade or so, numerous advances in the chemical synthesis of gold nanoparticles that are *not* spherical, especially anisotropic shapes such as nanorods, have opened up even more possibilities for sensing and imaging applications, for several different reasons. First, gold nanorods typically display two plasmon bands (one in the visible and another either in visible or in near-infrared, NIR) that are tunable depending on the dimensions of the nanorod; these two bands correspond to short-axis (transverse) and long-axis (longitudinal) plasmon modes (Figures 1 and 2).[5,6,9−12] Thus, if one wanted gold nanoparticles to absorb at a certain wavelength or frequency of light in the visible or NIR, one could synthesize particles of appropriate shape. Second, anisotropic nanoparticles may have different chemical reactivity for different crystal faces.[10−12] This property may lead to new assembly strategies or chemical sensing strategies; for instance, the longitudinal plasmon band, but not the transverse, will red-shift upon end-to-end aggregation of gold nanorods.[13]

Chemical Synthesis of Gold Nanoparticles of Different Shapes and Sizes

Simple reduction of metal salts by reducing agents in a controlled fashion generally produces spherical nanoparticles, because spheres are the lowest-energy shape. Some of the most well-known and frequently used methods to synthesize spherical gold nanoparticles include (a) the Turkevich method (1951) involving the reduction of gold chloride by citrate to produce 15 nm gold particles in boiling water, (b) the related Frens method (1973), (c) the Brust method (1994) for smaller (~2 nm) gold nanoparticles, in which an aqueous solution of gold ions is transferred to an organic phase, mediated by a phase transfer agent, followed by reduction with borohydride, (d) the microemulsion method wherein gold salts are reduced in the aqueous core of inverse micelles, and (e) the seeding method that we and others use, in which gold seed particles (prepared by one of the other methods) are used to grow more gold in the presence of a weak reducing agent.[10] For detailed procedures, readers are advised to see refs 7−11. Studies on growth kinetics and proposed mechanisms of anisotropic growth for metal nanorods have been documented elsewhere.[6−26] We also note that silica nanospheres with a nanoscale overcoat of gold ("nanoshells") also have tunable

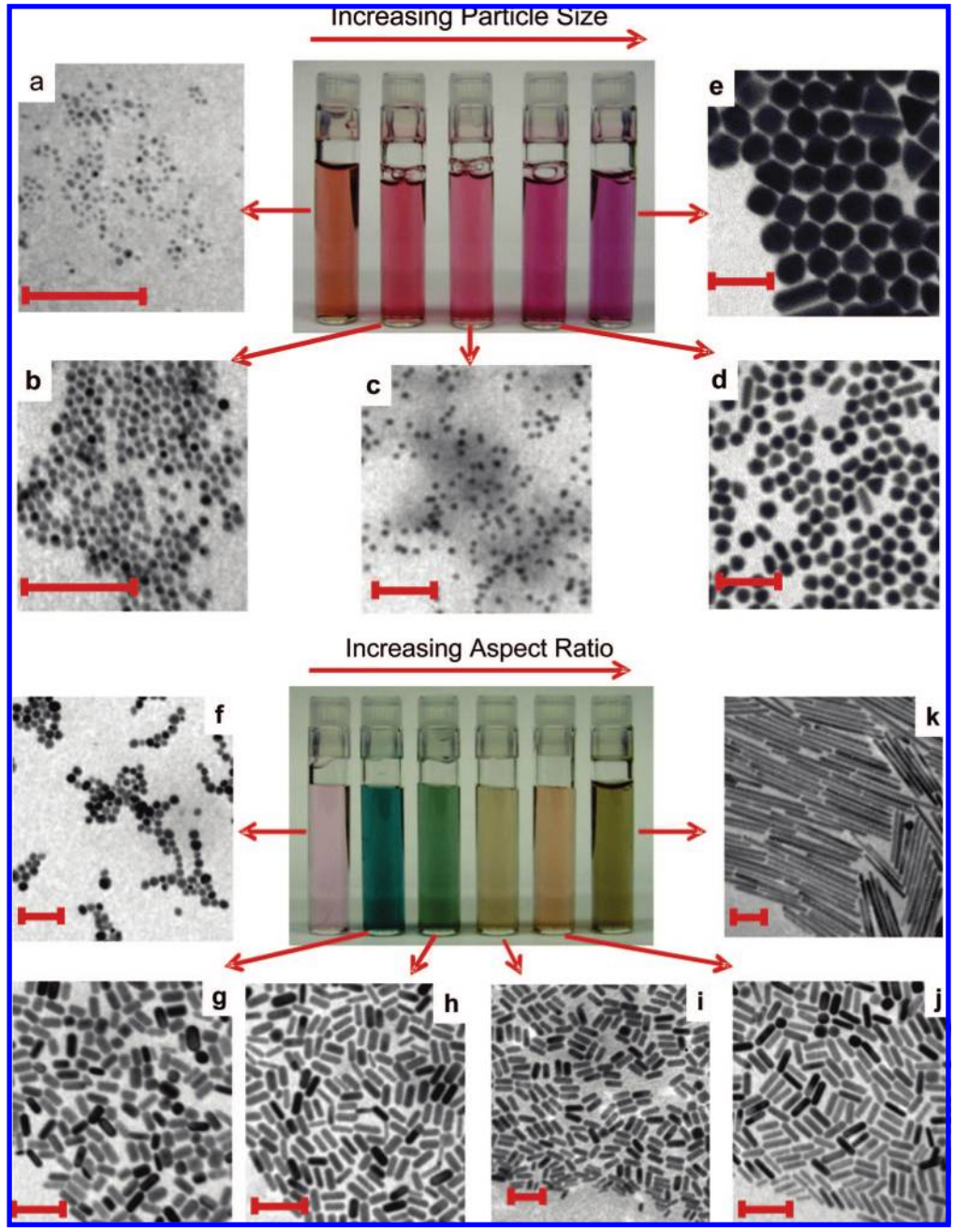

FIGURE 1. Photographs of aqueous solutions of gold nanospheres (upper panels) and gold nanorods (lower panels) as a function of increasing dimensions. Corresponding transmission electron microscopy images of the nanoparticles are shown; all scale bars = 100 nm. The difference in color of the particle solutions is more dramatic for rods than for spheres. This is due to the nature of plasmon bands (one for spheres and two for rods) that are more sensitive to size for rods compared with spheres. For spheres, the size varies from 4 to 40 nm (TEMs a−e), whereas for rods, the aspect ratio varies from 1.3 to 5 for short rods (TEMs f−j) and 20 (TEM k) for long rods.

absorption in the visible and NIR, and these materials are the subject of another recent review.[27]

How Toxic Are Gold Nanoparticles?

Potential applications of gold nanoparticles in biomedicine include chemical sensing and imaging applications.[6−12] While bulk gold has been deemed "safe", nanoscale particles of gold need to be examined for biocompatibility and environmental impact if they are to be manufactured on a large scale for *in vivo* usage.[28,29] Several groups have examined the cellular uptake and cellular toxicity (cytotoxicity) of gold nanoparticles. While nearly anything can be toxic at a high enough dose, the more relevant question is: how toxic are gold nanoparticles at the potential concentrations at which they might be used (which we estimate to be ~1−100 per cell)?[30] At present, relatively few reports have appeared in the primary literature.

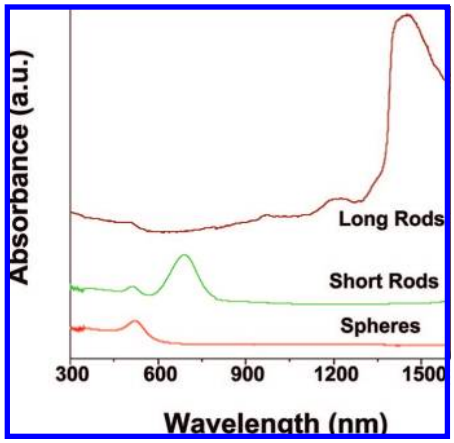

FIGURE 2. Optical spectra of gold nanoparticles of various shapes, showing positions of the plasmon bands. The sphere diameter is 8 nm; aspect ratio of the short rods is 3; aspect ratio of the long rods is 20.

We have examined the uptake and potential toxicity of a series of gold nanoparticles in human leukemia cells.[30] The nanoparticle library consisted of gold nanospheres that varied in both size (4, 12, and 18 nm diameter) and surface modifier. The surface modifiers included a range of anionic, neutral, and cationic groups: citrate, cysteine, glucose, biotin (aka vitamin B7 or H), and cetyltrimethylammonium bromide (CTAB). CTAB is the structure-directing agent that we use to control gold nanorod shape, and it appears to form a tightly bound cationic bilayer on gold nanoparticles, with the cationic trimethylammonium headgroup exposed to the solvent.[31,32] The K562 leukemia cell line was exposed to the nanoparticles for three days, at which time the cell viability was determined using a colorimetric MTT assay, which measures mitochondrial activity in viable cells. The data (Figure 3) suggested that none of the spherical gold nanoparticles were toxic to the human leukemia cells up to ~100 μM in gold atom concentration, even though they were being taken up into the cells (confirmed by transmission electron microscopy of cell slices). Similar viability studies with immune system cells also showed that gold nanoparticles were not cytotoxic and that they reduced the amount of potentially harmful reactive oxygen species in the cells.[29] However, we did find that the nanoparticle precursors, CTAB and the gold salt $HAuCl_4$, were toxic to the cells at ~10 nM concentrations.[30] Free CTAB (which may result from incomplete purification of the gold nanorods or desorption from the bound bilayer) is expected to be toxic to cells, because it is a detergent that can break open cell membranes.[30] Hence, proper purification of the gold nanorods will be a key step for any *in vivo* work.

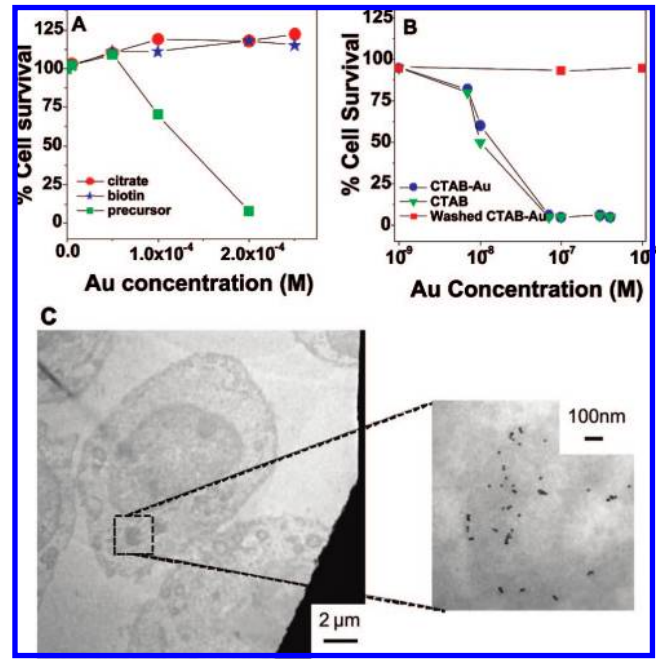

FIGURE 3. Human K562 cell survival data upon exposure to gold nanoparticles (cell exposure = 3 days; cell viability measured by MTT assay): (A) survival of cells exposed to 18 nm citrate-capped (red circle) or biotin-capped (blue star) gold nanospheres and to the $HAuCl_4$ precursor (green squares)—concentrations are in gold atoms and range from 0 to 2.5×10^{-4} M (corresponding to 0–1.4 nM in particles); (B) survival of cells exposed to unpurified 18 nm CTAB-capped gold nanospheres (blue spheres), purified 18 nm CTAB-capped gold nanospheres (red squares), and CTAB alone (green triangles)—concentrations range from nanomolar to micromolar in gold atoms for the particles, in molecules for CTAB; (C) transmission electron micrographs show the cells with gold nanoparticles. The image on the right is the high magnification image of a small region in the cell cytoplasm containing gold nanoparticles. Original data are from ref 30.

Other laboratories have investigated the cellular toxicity of gold nanoparticles with regard to particle size, shape, and surface group (Table 1).

Rotello et al. have investigated the toxicity of 2 nm gold nanoparticles functionalized with both cationic and anionic surface groups in three different cell types.[33] The results suggested that cationic particles are generally toxic at much lower concentrations than anionic particles, which they relate to the electrostatic interaction between the cationic nanoparticles and the negatively charged cell membranes.[33] Chan et al. have examined the uptake of gold nanoparticles of various sizes and shapes into HeLa cells, a well-known line of human cervical cancer cells.[34] They did not examine toxicity but did measure absolute gold concentrations in the cells by digestion and subsequent inductively coupled plasma atomic emission spectroscopy. They found that 50 nm spheres were taken up more quickly by the cells compared with both smaller and larger spheres in the 10–100 nm range and that spheres

TABLE 1. Summary of Selected Cytotoxicity Date for Gold Nanoparticles, 2004−2007

author	size (nm)	shape	surface group	cell line	toxicity results
Shukla[29]	3.5 ± 0.7	sphere	lysine, poly(L-lysine)	RAW264.7 mouse macrophage cells	85% cell viability after being exposed to 100 μM gold nanoparticles for 72 h
Connor[30]	4, 12, 18	sphere	citrate, cysteine, glucose, biotin, CTAB	K562 human leukemia	none of the spherical nanoparticles were toxic at the micromolar ranges used
Goodman[33]	2	sphere	quaternary ammonium, carboxylic acid	COS-1 mammalian cells, mammalian red blood cells, *Escherichia coli*	cationic nanoparticles were found to be much more toxic than anionic particles of the same size
Niidome[35]	65 ± 5 × 11 ± 1	rod	CTAB, PEG	HeLa cells	80% cell death with 0.05 mM CTAB-coated nanorods, only 10% cell death at 0.5 mM PEG-coated nanorods
Huff[36]		rod	CTAB	human tumor KB cells	gold nanoparticles were rapidly taken into the cells and formed permanent aggregates, but the cells remained healthy
Patra[41]	33	sphere	CTAB, citrate	BHK21 baby hamster kidney cells, Hep2G human liver carcinoma cells, A549 human carcinoma lung cells	nontoxic to BHK21 and HepG2 cells, but toxic to A549 cells
Takahashi[37]	65 × 11	rod	phosphatidyl-choline	HeLa cells	phosphatidylcholine-modified gold nanorods were much less toxic than CTAB-coated nanorods
Khan[39]	18	sphere	citrate	HeLa cells	gold nanoparticles did not cause significant gene-expression patterns or cyotoxicity even though they were internalized in the cells.

were taken up more efficiently than nanorods that had dimensions in the 10−100 nm range.[34]

In contrast to our results with CTAB-capped gold nanospheres, it has been reported that CTAB-capped gold nanorods are cytotoxic, as judged by the MTT assay with a different cell line, HeLa cells.[35] However, this group was able to reduce cytotoxicity by overcoating the nanorods with poly(ethylene glycol) (PEG), which is well-known to reduce nonspecific binding of biological molecules to surfaces.[35] Analogous cellular uptake experiments showed that the uptake of PEG-coated gold nanorods was only 6% relative to the original CTAB-coated gold nanorods.[36] Phosphatidylcholine is another biocompatible overcoating molecule that reduces the reported cytotoxicity of CTAB-coated gold nanorods.[37] Free CTAB, we believe, is the likely culprit in these toxicity assays, rather than the gold nanorods per se. More recently Chan et al. have reported that gold nanorods coated with CTAB and subsequently overcoated with polyelectrolytes show 90% cell viability for HeLa cells and cause little change in levels of gene expression: only 35 out of 10 000 genes examined were mildly down-regulated.[38] These results are similar to that of Khan et al. for 18 nm citrate-capped gold nanospheres.[39]

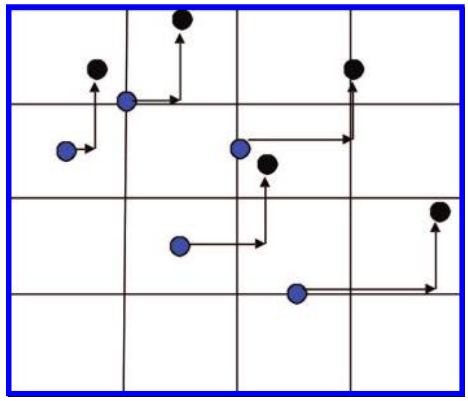

FIGURE 4. Illustration of digital image correlation. Blue dots denote positions of pattern markers within the sample before deformation. After deformation, the pattern positions are denoted by black dots. This mapping allows the measure of displacement.

It is important to differentiate between cytotoxicity and cellular damage. Nanoparticles that show little or no cytotoxicity via several standard assays may be still able to cause serious cellular damage. For example, 13 nm citrate-capped gold nanospheres were not toxic according to an assay in skin cells, but the particles did apparently promote the formation

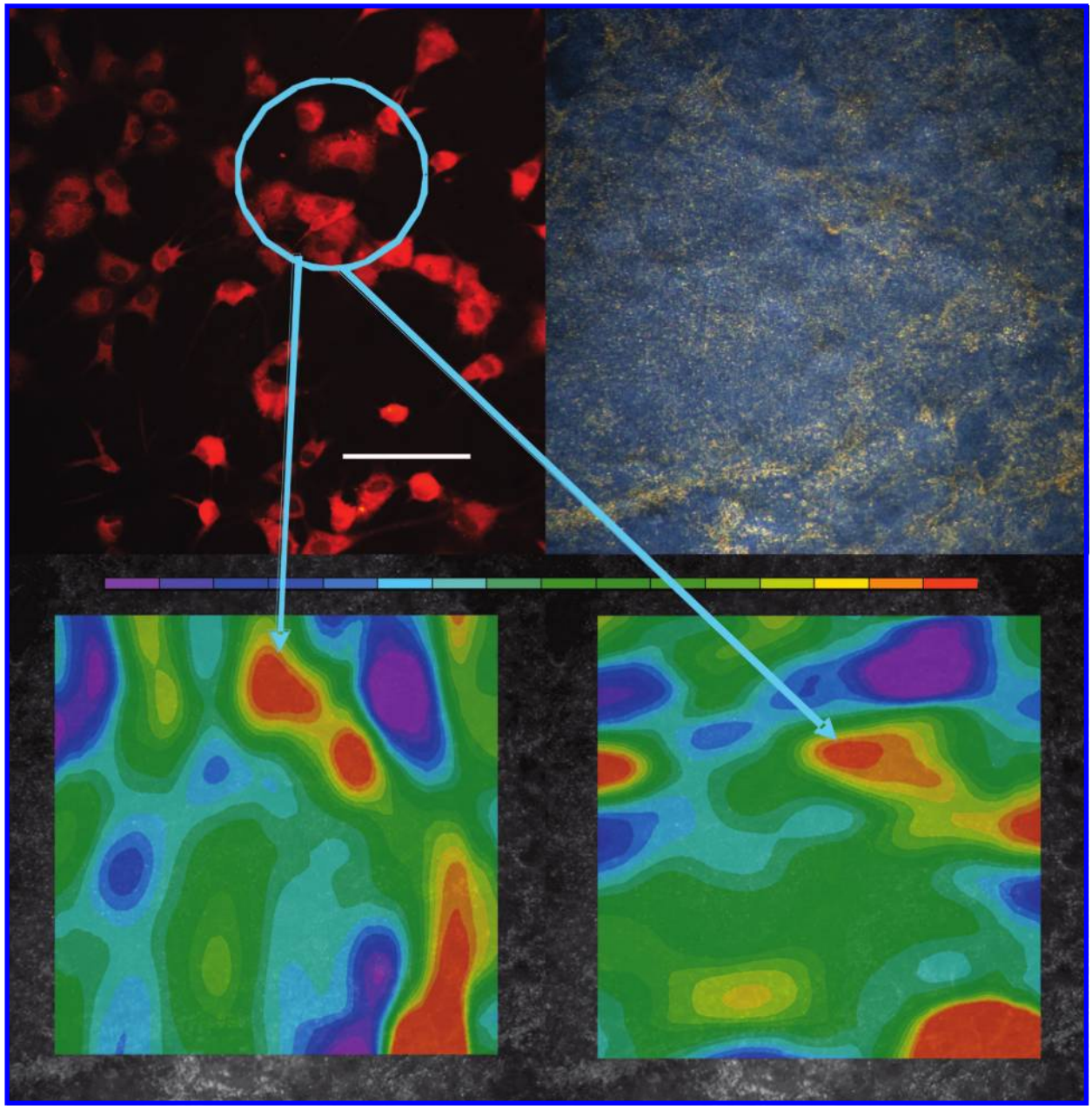

FIGURE 5. Fluorescently stained cardiac fibroblasts (top left); scale bar = 100 μm. Gold nanorods are present but are not visible by fluorescence. In the same sample but imaged by dark-field optical microscopy, gold nanorods (top right) scatter orange-yellow light. Contour plots are of (bottom left) horizontal strain, ε_{xx}, and (bottom right) vertical strain, ε_{yy}. The colored scale bar goes from compressive strain of −0.12 (purple) to tensile strain of 0.15 (red). The circled region shows that where there was extensive cell movement that deformed the matrix, significant vertical (ε_{yy}) and horizontal (ε_{xx}) strains are calculated.

of abnormal actin filaments, which led to decreases in cell proliferation, adhesion, and motility.[40]

Cytotoxicity also depends on the type of cells used. For example, 33 nm citrate-capped gold nanospheres were found to be noncytotoxic to baby hamster kidney and human hepatocellular liver carcinoma cells, but cytotoxic to a human carcinoma lung cell line at certain concentrations.[41] A recent excellent review summarizes data on cytotoxicity of nanoparticles for many types of materials.[42]

Cellular Imaging Using the Plasmon Bands of Gold Nanorods

The plasmons of metal nanoparticles enable one to image individual particle location with optical microscopy.[43−57] Two main imaging modalities have been demonstrated: dark-field optical microscopy and two-photon luminescence microscopy. Two-photon luminescence (TPL), which is thought to arise from coupling of weak electronic transitions in the metal to the plas-

mons in a nanoparticle, relies on the NIR properties of metallic nanorods.[58] Implemented as a microscopy experiment, which requires femtosecond laser pulses, TPL has been used to image the location of individual gold nanorods as they flow in blood *in vivo* and as they target cancer cells by virtue of the proper surface chemistry.[59,60] In dark-field optical microscopy, transmitted steady-state white light is blocked so that only steady-state scattered light is detected.[43−57] Because the scattering propagates as a cone, the spot size is much larger than the nanoparticle itself. Spatial resolution of ~200 nm is achievable, and single particles can be imaged.[43−57] Gold nanorods, compared with nanospheres, absorb intensely in the visible and NIR as a function of nanorod dimension (Figure 2).

We have taken advantage of this ability to "see" where the nanorods are via optical dark-field microscopy and use it as the basis for measuring local deformations in optically transparent materials. As a material is deformed under a mechanical load, the embedded nanorods, visible as "points of light" in the microscope, move. Matching the original pattern of light to the deformed pattern allows us to track small scale, potentially heterogeneous, deformations throughout the material.

We use the movement of gold nanorods to observe material response under loading. The response we measure is displacement, with a resolution of ~200 nm; strain, which is a gradient of displacement, can then be numerically approximated from the displacement field. Engineering normal strain is defined as the change in length of a line divided by its original length, $\Delta L/L$, and can be calculated in all three coordinate directions. Strain is a dimensionless quantity; by convention, if a material is lengthened, strain is positive (tension); if a material is shortened, strain is negative (compression). Strain occurs in response to mechanical load, mathematically defined by stress, force applied per unit area. Constitutive laws establish relationships between stress and strain, for example, stiffness, which is the change in stress per change in strain, or toughness, which is the strain energy absorption, obtained from the area underneath a stress/strain curve.[61]

To measure displacements, an image correlation analysis is used. This analysis matches a digital image of a surface before loading, *the undeformed image*, to an image taken of the surface after loading, *the deformed image*. The surface must have a visibly distinguishable pattern, either applied or inherent, where different pixels have different gray scale intensities. The underlying concept is very simple (Figure 4). If an individual point (x, y) in the first image can be matched to its new location $(\hat{x}, \hat{y})$ in a second image, then the displacement of the point is $(u, v) = (\hat{x} - x, \hat{y} - y)$. The resulting displacement field will show the relative movement of the material, stiffer regions moving less than compliant regions under the same load, and characterize the material's response. The difficulty lies in tracking each pixel from its location in the undeformed image to its new position after deformation. The image correlation software VIC-2D (Correlated Solutions) uses a correlation function to compare the light intensities locally surrounding each pixel and efficiently search the deformed image for the best match.[62−66]

For proof of concept experiments, our group used gold nanorods (372 nm average length, and 23 nm average width) embedded in poly(vinyl alcohol) (PVA) or polydimethylsiloxane (PDMS) to track deformations in the polymers as the films were longitudinally stretched.[67] Because the stretching was done on relatively homogeneous materials, we compared the measurements made by tracking the nanorods to a bulk approximation for engineering strain, $\Delta L/L$. The longitudinal strain, averaged over the full field of view calculated by using the nanorods, corresponded well to the global bulk estimate.[67]

Potentially more useful is the capability of measuring the deformation of a material expected to be locally heterogeneous, for example, soft biological tissue constructs. At the cellular and smaller scales, these materials display significant heterogeneity, so a complete characterization requires field measurements of mechanical response over a representative area, rather than a single averaged bulk response.

Cells are influenced, by external loads or endogenous forces, through physical connections to their extracellular matrix (ECM), which in cardiac tissue mainly consists of the protein collagen.[61,68−74] These loads produce local heterogeneous deformations (strains) largely as a result of the locally varying material properties of the ECM network (density, microstructure, organization, etc.). The cell's perception of the local mechanical environment triggers biophysical and biochemical responses, which can result in adaptive changes to the mechanical properties of the ECM and alter the cell's local mechanical environment. Thus, a complex feedback loop is used to maintain tissue homeostasis under functional needs. A number of groups have used microbeads to examine how single cells deform their surroundings;[72,75,76] we have complemented these studies by using gold nanorods as nonbleaching optical markers to examine local, cell-induced ECM deformation that occurs between living cells.[77]

In our work, gold nanorods were added to thin collagen films and subsequently plated with neonatal cardiac fibroblasts, the cells responsible for depositing and modifying the ECM. Cells were stained with a fluorescent dye and could be

imaged nearly simultaneously with the scattering from gold nanorods in a combination fluorescence−dark-field optical microscope (Figure 5).

The positional displacements of the gold nanorods, generated by the traction forces applied by the cells through their attachments to the ECM, were tracked, and strain fields were calculated from the displacements (Figure 5). Clearly, strains across the field of view are inhomogeneous (tension is red; compression is blue) suggesting either varying material properties or varied localized application of force by the cells. These results are consistent with other work on sparsely populated collagen matrices[78] and provide data that will enable improved understanding of the biomechanical feedback loops that cells use.

Prospects for the Future

Gold nanorods are an attractive alternative to traditional organic fluorescent dyes in that they do not photobleach, they can absorb throughout the visible and NIR, and they can be nontoxic under certain experimental conditions. We envision, in the next 5 years, intensive research activity focused on the *in vivo* uses of gold nanoparticles. There is already a healthy amount of work on *in vitro* diagnostics. Most of the activity, we project, will be tied to specific detection, imaging, and therapy for very particular target cells (e.g., certain cancers, bacteria). In parallel and for each study, toxicity and side effects need to be thoroughly examined in the broadest possible context, as a function of nanoparticle size, shape, and surface coating, beyond simple cell lines, before human subjects can be exposed to these materials.

Have we learned anything new in biology because of these nanomaterials? The answer, with several exceptions, is not really, yet. Once the biomedical community embraces gold nanoparticles as new tools for *in vivo* imaging, for longer time scales and with less background than current fluorescent probes, we speculate that new knowledge of how cells and organs work, both internally and externally with others, will be obtained. We envision, in the 5−10 year time frame, that increased collaboration between practitioners the fields of biology, medicine, nanoscience, and nanotechnology will yield new fundamental insights into biological systems.

We thank past and present members of our research team for their work. We especially thank Prof. C. Robinson for his contributions to imaging. We gratefully acknowledge support from the National Science Foundation, W. M. Keck Foundation, and the University of South Carolina.

BIOGRAPHICAL INFORMATION

Catherine J. Murphy was born in New Jersey and grew up in suburban Chicago. She received two B.S. degrees (chemistry and biochemistry) from the University of Illinois at Urbana−Champaign, followed by a Ph.D. in chemistry from the University of Wisconsin—Madison. She was a postdoctoral fellow at the California Institute of Technology before getting her first real job at the University of South Carolina, where she is presently the Guy F. Lipscomb Professor of Chemistry.

Anand M. Gole was born in Bhavnagar, India, and obtained B.Sc. and M.Sc. degrees from the University of Pune, India. Upon completion of his Ph.D. at National Chemical Laboratory, Pune, he worked as a postdoctoral researcher (France and US) and as a Senior Scientist (Singapore). Currently he is a Research Assistant Professor at the University of South Carolina with research interests in bionanotechnology.

John W. Stone is a native of Savannah, Georgia, and received his B.S. degree in chemistry from Armstrong Atlantic State University there. He is currently a Ph.D. student at the University of South Carolina with Profs. Murphy, Baxter, and Goldsmith.

Patrick N. Sisco is a native of Savannah, Georgia, and received his B.S. degree in chemistry from Armstrong Atlantic State University there. He is currently a Ph.D. student at the University of South Carolina with Profs. Murphy, Baxter, and Goldsmith.

Alaaldin M. Alkilany was born in Irbid, Jordan. He earned his B.Sc. in pharmacy from Jordan University of Science and Technology. He was a formulation scientist in the R&D department of Hikma Pharmaceuticals in Jordan before joining the Murphy group as a Ph.D. student at the University of South Carolina.

Edie C. Goldsmith was born in San Diego and received her B.S. in biochemistry from the College of Charleston in Charleston, South Carolina. She earned a Ph.D. in chemistry from the University of North Carolina—Chapel Hill. After postdoctoral work at the University of South Carolina, she joined the faculty there as an Assistant Professor in the School of Medicine. Her research interests are in cell−extracellular matrix interactions in the developing heart.

Sarah C. Baxter is a native of Colorado. She received an M.S. in applied and computational mathematics from the University of Minnesota and a Ph.D. in applied mathematics from the University of Virginia. After postdoctoral work in applied mechanics, she was appointed to the faculty in Mechanical Engineering at the University of South Carolina, where she is currently an Associate Professor. Her research interests are in the mechanics of heterogeneous materials.

FOOTNOTES

*To whom correspondence should be addressed. E-mail: Murphy@mail.chem.sc.edu.

REFERENCES

1 Higby, G. J. Gold in Medicine. *Gold Bull.* **1982**, *15*, 130–140.

2 Wagner, F. E.; Haslbeck, S.; Stievano, L.; Calogero, S.; Pankhurst, Q. A.; Martinek, K.-P. Before Striking Gold in Gold-Ruby Glass. *Nature* **2000**, *407*, 691–692.

3 Edwards, P. P.; Thomas, J. M. Gold in a Metallic Divided State-From Faraday to Present-Day Nanoscience. *Angew. Chem., Int. Ed.* **2007**, *46*, 5480–5486.

4 Murphy, C. J. Nanocubes and Nanoboxes. *Science* **2002**, *298*, 2139–2141.

5 Kelly, K. L.; Coronado, E.; Zhao, L. L.; Schatz, G. C. The Optical Properties of Metal Nanoparticles: The Influence of Size, Shape, and Dielectric Environment. *J. Phys. Chem. B* **2003**, *107*, 668–677.

6 El-Sayed, M. A. Some Interesting Properties of Metals Confined in Time and Nanometer Space of Different Shapes. *Acc. Chem. Res.* **2001**, *34*, 257–264.

7 Daniel, M.-C.; Astruc, D. Gold Nanoparticles: Assembly, Supramolecular Chemistry, Quantum-Size-Related Properties, and Applications toward Biology, Catalysis, and Nanotechnology. *Chem. Rev.* **2004**, *104*, 293–346.

8 Rosi, N. L.; Mirkin, C. A. Nanostructures in Biodiagnostics. *Chem. Rev.* **2005**, *105*, 1547–1562.

9 Burda, C.; Chen, X.; Narayanan, R.; El-Sayed, M. A. Chemistry and Properties of Nanocrystals of Different Shapes. *Chem. Rev.* **2005**, *105*, 1025–1102.

10 Murphy, C. J.; Sau, T. K.; Gole, A. M.; Orendorff, C. J.; Gao, J.; Gou, L.; Hunyadi, S. E.; Li, T. Anisotropic Metal Nanoparticles: Synthesis, Assembly, and Optical Applications. *J. Phys. Chem. B.* **2005**, *109*, 13857–13870.

11 Murphy, C. J.; Gole, A. M.;.; Hunyadi, S. E.; Orendorff, C. J. One-Dimensional Colloidal Gold and Silver Nanostructures. *Inorg. Chem.* **2006**, *45*, 7544–7554.

12 Murphy, C. J.; Gole, A. M.; Hunyadi, S. E.; Stone, J. W.; Sisco, P. N.; Alkilany, A.; Kinard, B. E.; Hankins, P. Chemical Sensing and Imaging with Metallic Nanorods. *Chem. Commun.* **2008**, 544–557.

13 Thomas, K. G.; Barazzouk, S.; Ipe, B. I.; Joseph, S. T. S.; Kamat, P. V. Uniaxial Plasmon Coupling through Longitudinal Self-Assembly of Gold Nanorods. *J. Phys. Chem. B.* **2004**, *108*, 13066–13068.

14 Jana, N. R.; Gearheart, L.; Murphy, C. J. Wet Chemical Synthesis of High Aspect Ratio Gold Nanorods. *J. Phys. Chem. B* **2001**, *105*, 4065–4067.

15 Murphy, C. J.; Jana, N. R. Controlling the Aspect Ratio of Inorganic Nanorods and Nanowires. *Adv. Mater.* **2002**, *14*, 80–82.

16 Johnson, C. J.; Dujardin, E.; Davis, S. A.; Murphy, C. J.; Mann, S. Growth and Form of Gold Nanorods Prepared by Seed-Mediated, Surfactant-Directed Synthesis. *J. Mater. Chem.* **2002**, *12*, 1765–1770.

17 Xia, Y.; Yang, P.; Sun, Y.; Wu, Y.; Mayers, B.; Gates, B.; Yin, Y.; Kim, F.; Yan, H. One-Dimensional Nanostructures: Synthesis, Characterization, and Applications. *Adv. Mater.* **2003**, *15*, 353–389.

18 Nikoobakht, B.; El-Sayed, M. A. Preparation and Growth Mechanism of Gold Nanorods (NRs) Using Seed-Mediated Growth Method. *Chem. Mater.* **2003**, *15*, 1957–1962.

19 Perez-Juste, J.; Liz-Marzan, L. M.; Carnie, S.; Chan, D. Y. C.; Mulvaney, P. Electric-Field-Directed Growth of Gold Nanorods in Aqueous Surfactant Solutions. *Adv. Funct. Mater.* **2004**, *14*, 571–579.

20 Liao, H.; Hafner, J. H. Monitoring Gold Nanorod Synthesis on Surfaces. *J. Phys. Chem. B.* **2004**, *108*, 19276–19280.

21 Gole, A.; Murphy, C. J. Seed-Mediated Synthesis of Gold Nanorods: Role of the Size and Nature of the Seed. *Chem. Mater.* **2004**, *16*, 3633–3640.

22 Sau, T. K.; Murphy, C. J. Room Temperature, High-Yield Synthesis of Multiple Shapes of Gold Nanoparticles in Aqueous Solution. *J. Am. Chem. Soc.* **2004**, *126*, 8648–8649.

23 Kim, F.; Connor, S.; Song, H.; Kuykendall, T.; Yang, P. Platonic Gold Nanocrystals. *Angew. Chem., Int. Ed.* **2004**, *43*, 3673–3677.

24 Perez-Juste, J.; Pastoriza-Santos, I.; Liz-Marzan, L. M.; Mulvaney, P. Gold Nanorods: Synthesis, Characterization and Applications. *Coord. Chem. Rev.* **2005**, *249*, 1870–1901.

25 Zhang, J.; Liu, H.; Wang, Z.; Ming, N. Shape-Selective Synthesis of Gold Nanoparticles with Controlled Sizes, Shapes, and Plasmon Resonances. *Adv. Funct. Mater.* **2007**, *17*, 3295–3303.

26 Jiang, X. C.; Pileni, M. P. Gold Nanorods: Influence of Various Parameters as Seeds, Solvent, Surfactant on Shape Control. *Colloids Surf. A.* **2007**, *295*, 228–232.

27 Hirsch, L. R.; Gobin, A. M.; Lowery, A. R.; Tam, F.; Drezek, R. A.; Halas, N. J.; West, J. L. Metal Nanoshells. *Ann. Biomed. Eng.* **2006**, *34*, 15–22.

28 Colvin, V. The Potential Environmental Impact of Engineered Nanomaterials. *Nat. Biotechnol.* **2003**, *21*, 1166–1170.

29 Shukla, R.; Bansal, V.; Chaudhary, M.; Basu, A.; Bhonde, R.; Sastry, M. Biocompatibility of Gold Nanoparticles and Their Endocytotic Fate Inside the Cellular Compartment: A Microscopic Overview. *Langmuir* **2005**, *21*, 10644–10654.

30 Connor, E. E.; Mwamuka, J.; Gole, A.; Murphy, C. J.; Wyatt, M. D. Gold Nanoparticles Are Taken Up by Human Cells but Do Not Cause Acute Cytotoxicity. *Small* **2005**, *1*, 325–327.

31 Nikoobakht, B.; El-Sayed, M. A. Evidence for Bilayer Assembly of Cationic Surfactants on the Surface of Gold Nanorods. *Langmuir* **2001**, *17*, 6368–6374.

32 Sau, T. K.; Murphy, C. J. Self-Assembly Patterns Formed Upon Solvent Evaporation of Aqueous Cetyltrimethylammonium Bromide-Coated Gold Nanoparticles of Various Shapes. *Langmuir* **2005**, *21*, 2923–2929.

33 Goodman, C. M.; McCusker, C. D.; Yilmaz, T.; Rotello, V. M. Toxicity of Gold Nanoparticles Functionalized with Cationic and Anionic Side Chains. *Bioconjugate Chem.* **2004**, *15*, 897–900.

34 Chithrani, B. D.; Ghazani, A. A.; Chan, W. C. W. Determining the Size and Shape Dependence of Gold Nanoparticle Uptake into Mammalian Cells. *Nano Lett.* **2006**, *6*, 662–668.

35 Niidome, T.; Yamagata, M.; Okamoto, Y.; Akiyama, Y.; Takahashi, H.; Kawano, T.; Katayama, Y.; Niidome, Y. PEG-Modified Gold Nanorods with a Stealth Character for in Vivo Applications. *J. Controlled Release* **2006**, *114*, 343–347.

36 Huff, T. B.; Hansen, M. N.; Zhao, Y.; Cheng, J. X.; Wei, A. Controlling the Cellular Uptake of Gold Nanorods. *Langmuir* **2007**, *23*, 1596–1599.

37 Takahashi, H.; Niidome, Y.; Niidome, T.; Kaneko, K.; Kawasaki, H.; Yamada, S. Modification of Gold Nanorods Using Phosphatidylcholine to Reduce Cytotoxicity. *Langmuir* **2006**, *22*, 2–5.

38 Hauck, T. S.; Ghazani, A. A.; Chan, W. C. W. Assessing the Effect of Surface Chemistry on Gold Nanorod Uptake, Toxicity, and Gene Expression in Mammalian Cells. *Small* **2008**, *4*, 153–159.

39 Khan, J. A.; Pillai, B.; Das, T. K.; Singh, Y.; Maiti, S. Molecular Effects of Gold Nanoparticles in HeLa Cells. *ChemBioChem* **2007**, *8*, 1237–1240.

40 Pernodet, N.; fang, X.; Sun, Y.; Bakhtina, A.; Ramakrishnan, A.; Sokolov, J.; Ulman, A.; Rafailovich, M. Adverse Effects of Citrate/Gold Nanoparticles on Human Dermal Fibroblasts. *Small* **2006**, *6*, 766–773.

41 Patra, H. K.; Banerjee, S.; Chaudhuri, U.; Lahiri, P.; Dasgupta, A. K. Cell-Selective Response to Gold Nanoparticles. *Nanomedicine* **2007**, *3*, 111–119.

42 Lewinski, N.; Colvin, V.; Drezek, R. Cytotoxicity of Nanoparticles. *Small* **2008**, *4*, 26–49.

43 Schultz, S.; Smith, D. R.; Mock, J. J.; Schultz, D. A. Single-Target Molecule Detection with Nonbleaching Multicolor Optical Immunolabels. *Proc. Natl. Acad. Sci. U.S.A.* **2000**, *97*, 996–1001.

44 Xu, X-H. N.; Chen, J.; Jeffers, R. B.; Kyriacou, S. Direct Measurement of Sizes and Dynamics of Single Living Membrane Transporters Using Nanooptics. *Nano Lett.* **2002**, *2*, 175–182.

45 McFarland, A. D.; Van Duyne, R. P. Single Silver Nanoparticles as Real-Time Optical Sensors with Zeptomole Sensitivity. *Nano Lett.* **2003**, *3*, 1057–1062.

46 Mock, J. J.; Smith, D. R.; Schultz, S. Local Refractive Index Dependence of Plasmon Resonance Spectra from Individual Nanoparticles. *Nano Lett.* **2003**, *3*, 485–491.

47 Raschke, G.; Kowarik, S.; Franzl, T.; Sonnichsen, C.; Klar, T. A.; Feldmann, J.; Nichtl, A.; Kurzinger, K. Biomolecular Recognition Based on Single Gold Nanoparticle Light Scattering. *Nano Lett.* **2003**, *3*, 935–938.

48 Prikulis, J.; Svedberg, F.; Kall, M.; Enger, J.; Ramser, K.; Goksor, M.; Hanstorp, D. Optical Spectroscopy of Single Trapped Metal Nanoparticles in Solution. *Nano Lett.* **2004**, *4*, 115–118.

49 Xu, X-H. N.; Brownlow, W. J.; Kyriacou, S. V.; Wan, Q.; Viola, J. J. Real-Time Probing of Membrane Transport in Living Microbial Cells Using Single Nanoparticle Optics and Live Cell Imaging. *Biochemistry* **2004**, *43*, 10400–10413.

50 Sonnichsen, C.; Alivisatos, A. P. Gold Nanorods as Novel Nonbleaching Plasmon-Based Orientation Sensors for Polarized Single Particle Spectroscopy. *Nano Lett.* **2005**, *5*, 301–304.

51 El-Sayed, I. H.; Huang, X.; El-Sayed, M. A. Surface Plasmon Resonance Scattering and Absorption of anti-EGFR Antibody Conjugated Gold Nanoparticles in Cancer Diagnostics: Applications in Oral Cancer. *Nano Lett.* **2005**, *5*, 829–834.

52 Sonnichsen, C.; Reinhard, B. M.; Liphardt, J.; Alivisatos, A. P. A Molecular Ruler Based on Plasmon Coupling of Single Gold and Silver Nanoparticles. *Nat. Biotechnol.* **2005**, *23*, 71–745.

53 Huang, X.; El Sayed, E. H.; Qian, W.; El Sayed, M. A. Cancer Cell Imaging and Photothermal Therapy in the Near-Infrared Region by Using Gold Nanorods. *J. Am. Chem. Soc.* **2006**, *128*, 2115–2120.

54 Orendorff, C. J.; Sau, T. K.; Murphy, C. J. Shape-Dependent Plasmon-Resonant Gold Nanoparticles. *Small* **2006**, *2*, 636–639.

55 Kumar, S.; Harrison, N.; Richards-Kortum, R.; Sokolov, K. Plasmonic Nanosensors for Imaging Intracellular Biomarkers in Live Cells. *Nano Lett.* **2007**, *7*, 1338–1343.

56 Nehl, C. L.; Liao, H. W.; Hafner, J. H. Optical Properties of Star-Shaped Gold Nanoparticles. *Nano Lett.* **2006**, *6*, 683–688.

57 Hasan, W.; Lee, J.; Henzie, J.; Odom, T. W. Selective Functionalization and Spectral Identification of Gold Nanopyramids. *J. Phys. Chem. C* **2007**, *111*, 17176–17179.

58 Imura, K.; Nagahara, T.; Okamoto, H. Plasmon Mode Imaging of Single Gold Nanorods. *J. Am. Chem. Soc.* **2004**, *126*, 12730–12731.

59 Wang, H. F.; Huff, T. B.; Zweifel, D. A.; He, W.; Low, P. S.; Wei, A.; Cheng, J. X. In

vitro and in Vivo Two-Photon Luminescence Imaging of Single Gold Nanorods. *Proc. Natl. Acad. Sci. U.S.A.* **2005**, *102*, 15752–15756.

60 Durr, N. J.; Larson, T.; Smith, D. K.; Korgel, B. A.; Sokolov, K.; Ben-Yakar, A. Two-Photon Luminescence Imaging of Cancer Cells Using Molecularly Targeted Gold Nanorods. *Nano Lett.* **2007**, *7*, 941–945.

61 Silver, F. H. *Mechanosensing and Mechanochemical Tranduction in Extracellular Matrix*; Springer: New York, 2006.

62 Sutton, M. A.; Wolters, W. J.; Peters, W. H.; Ranson, W. F.; McNeill, S. R. Determination of Displacements Using an Improved Digital Correlation Method. *Image Vision Computing* **1983**, *1*, 133–139.

63 Chu, T. C.; Ranson, W. F.; Sutton, M. A.; Peters, W. H. Applications of Digital Image Correlation Techniques to Experimental Mechanics. *Exp. Mech.* **1985**, *25*, 232–244.

64 Sutton, M. A.; Cheng, M.; Peters, W. H.; Chao, Y. J.; McNeill, S. R. Application of an Optimized Digital Image Correlation Method to Planar Deformation Analysis. *Image Vision Computing* **1986**, *4*, 143–150.

65 Sutton, M. A.; McNeill, S. R.; Jang, J.; Babai, M. The Effect of Subpixel Image Resaturation on Digital Image Correlation Estimates. *Opt. Eng.* **1988**, *27*, 870–877.

66 Helm, J. D.; McNeill, S. R.; Sutton, M. A. Improved 3-D Image Correlation for Surface Displacement Measurement. *Opt. Eng.* **1996**, *35*, 1911.

67 Orendorff, C. J.; Baxter, S. C.; Goldsmith, E. C.; Murphy, C. J. Light Scattering from Gold Nanorods: Tracking Material Deformation. *Nanotechnology* **2005**, *16*, 2601–2605.

68 Zhu, C.; Bao, G.; Wang, N. Cell Mechanics: Mechanical Response, Cell Adhesion and Molecular Deformation. *Annu. Rev. Biomed. Engr.* **2000**, *2*, 189–226.

69 Humphrey, J. D. Stress, Strain, and Mechanotransduction in Cells. *J. Biomech. Eng., Trans. ASME* **2001**, *123*, 638–641.

70 Roeder, B. A.; Kokini, K.; Robinson, J. P.; Voytik-Harbin, S. L. Local, Three-Dimensional Strain Measurements Within Largely Deformed Extracellular Matrix Constructs. *J. Biomech. Eng., Trans. ASME* **2004**, *126*, 699–708.

71 Grinnell, F. Fibroblast Biology in Three-Dimensional Collagen Matrices. *Trends Cell Biol.* **2003**, *13*, 264–269.

72 Wang, N.; Ostuni, E.; Whitesides, G. M.; Ingber, D. E. Micropatterning Tractional Forces in Living Cells. *Cell Motil. Cytoskeleton* **2002**, *33*, 469–1490.

73 Swartz, M. A.; Tshumperlin, D. J.; Kamm, R. D.; Drazen, J. M. Mechanical Stress is Communicated between Different Cell Types to Elicit Matrix Remodeling. *Proc. Natl. Acad. Sci. U.S.A.* **2001**, *98*, 6180–6185.

74 Bischofs, I. B.; Schwarz, U. S. Cell Organization in Soft Media due to Active Mechano-sensing. *Proc. Natl. Acad. Sci. U.S.A.* **2003**, *100*, 9274–9279.

75 Butler, J. P.; Tolic-Norrelykke, I. M.; Fabry, B.; Fredberg, J. J. Traction Fields, Moments, and Strain Energy that Cells Exert on Their Surroundings. *Am. J. Physiol. Cell Physiol.* **2002**, *282*, C595–C605.

76 Tolic-Norrelykke, I. M.; Wang, N. Traction in Smooth Muscle Cells Varies with Cell Spreading. *J. Biomech.* **2005**, *38*, 1405–1412.

77 Stone, J. W.; Sisco, P. N.; Goldsmith, E. C.; Baxter, S. C.; Murphy, C. J. Using Gold Nanorods to Probe Cell-Induced Collagen Deformation. *Nano Lett.* **2007**, *7*, 116–119.

78 Vanni, S.; Lagerholm, C.; Otey, C.; Taylor, D. L.; Lanni, F. Internet-Based Image Analysis Quantifies Contractile Behavior of Individual Fibroblasts inside Model Tissue. *Biophys. J.* **2003**, *84*, 2715–2727.